

COMMUNICATION

Mice lacking endogenous TRPV1 express reduced levels of thermogenic proteins and are susceptible to diet-induced obesity and metabolic dysfunction

Padmamalini Baskaran, Kara Nazminia, Justine Frantz, Jessica O'Neal and Baskaran Thyagarajan 

Molecular Signaling Laboratory, School of Pharmacy, University of Wyoming, Laramie, WY, USA

Correspondence

B. Thyagarajan, Molecular Signaling Laboratory College of Health Sciences - School of Pharmacy, University of Wyoming, HS 279, Dept. 3375, 1000 East University Avenue, Laramie, WY 82071, USA

Tel: +1 (307) 766 6482 (Office);

+1 (307) 766 6147 (Lab)

E-mail: baskaran.thyagarajan@uwyo.edu

(Received 3 December 2020, revised 4 May 2021, accepted 5 May 2021, available online 30 May 2021)

doi:10.1002/1873-3468.14105

Edited by László Nagy

Transient receptor potential vanilloid subfamily 1 (TRPV1) is a non-selective cation channel protein expressed in neuronal and non-neuronal cells. Although TRPV1 is implicated in thermogenesis and diet-induced obesity (DIO), its precise role remains controversial. TRPV1^{-/-} mice are protected from DIO, while TRPV1 activation enhances thermogenesis to prevent obesity. To reconcile this, we fed wild-type and TRPV1^{-/-} mice for 32 weeks with normal chow or a high-fat diet and analyzed the weight gain, metabolic activities, and thermogenic protein expression in white and brown fats. TRPV1^{-/-} mice became obese, exhibited reduced locomotor activity, reduced energy expenditure, enhanced hepatic steatosis, and decreased thermogenic protein expression in adipose tissues. Our data reveal that lack of TRPV1 does not prevent obesity, but rather enhances metabolic dysfunction.

Keywords: adipose tissue; adiposity; fatty liver; metabolism; obesity; TRPV1^{-/-}

Transient receptor potential vanilloid 1 (TRPV1) is a member of the vanilloid subfamily of the TRP superfamily of proteins. TRPV1 is predominately expressed in the sensory nerve terminals, where it mediates thermal pain sensitization mechanisms. Recently, its expression and functions are recognized in non-neuronal tissues such as skeletal muscles, liver, and adipose tissues [1,2].

Published works suggest that TRPV1, also known as capsaicin receptor, is implicated in high-fat diet (HFD)-induced obesity [3–5]. TRPV1 prevents body-weight gain in HFD-fed mice [4]. TRPV1 is recognized as a promising target for countering diet-induced obesity [3,4,6–12]. This suggests that TRPV1 expression

and activation are important for the anti-obesity effect of capsaicin. However, the precise mechanism by which TRPV1 regulates metabolic activity remains unclear. Also, controversy exists in the role of TRPV1 in HFD-induced obesity. That is, published studies suggest that the lack of TRPV1 protects against HFD-induced obesity and metabolic pathologies [9,13,14]. On the other hand, studies suggest that TRPV1 activation by capsaicin prevents obesity and associated comorbidities [3,4,6,8]. Thus far previous research has not evaluated the differences among the thermogenic machinery (expression of proteins that regulate thermogenesis in adipose tissues) between WT and TRPV1^{-/-} mice. This research reconciles this by

Abbreviations

BAT, brown adipose tissue; BF, brown fat; BMP8b, bone morphogenetic protein 8b; EF, epididymal fat; GLP-1, glucagon-like peptide 1; HFD, high-fat diet; IPGTT, intraperitoneal glucose tolerance test; NAD⁺, nicotinamide adenine dinucleotide; NCD, normal chow diet; PPAR, peroxisome proliferator-activated receptor; PGC-1 α , PPAR gamma 1 coactivator; PRDM-16, PR domain containing 16; SIRT-1, sirtuin 1; TRPV1, transient receptor potential cation channel, subfamily V number 1; TRPV1^{-/-}, TRPV1 knockout; mtrpv1, mouse TRPV1; UCP-1, uncoupling protein 1; WAT, white adipose tissue; iWAT, inguinal WAT; sWAT, subcutaneous WAT; WT, wild-type.

evaluating the effect of feeding a normal chow diet (NCD) or an HFD for 32 weeks in the wild-type and TRPV1^{-/-} mice and by analyzing the expression of metabolically important genes/proteins in the white and brown fats.

Previous work suggests that HFD feeding suppresses the expression of TRPV1 and metabolically important adipogenic and thermogenic proteins in adipocytes [3,15] and dietary capsaicin reverses the inhibitory effect of HFD [3]. Further, capsaicin stimulates the browning of white adipose tissue by activating TRPV1 [3,6]. Although these observations indicate a central role of TRPV1 in regulating adipogenic and thermogenic mechanisms, it also raises an important question—whether the lack of endogenous TRPV1 expression modulates the expression profiles of adipogenic genes and thermogenic proteins? The results presented in this manuscript unequivocally demonstrate that the lack of TRPV1 endogenously does not protect mice from HFD-induced obesity, but rather promotes weight gain and metabolic dysfunction. These results will contribute toward broadening our knowledge on the role of TRPV1 in metabolic functions. Also, this article makes it clear that variations in the types of HFD used in published studies influence the outcome of the research. Collectively, the results presented here clarify that TRPV1 expression does play a role in the regulation of expression of adipogenic and thermogenic proteins in the white and brown fat isolated from NCD or HFD-fed mice. This knowledge will contribute to a broader understanding of the role of TRPV1 in the regulation of adipogenic and thermogenic mechanisms.

Materials and methods

Mouse model of high-fat diet-induced obesity

Adult male TRPV1^{-/-} (B6.129X1-*Trpv1*^{tm1Jul/J}) mice and their genetically unaltered control (wild-type, WT) mice were purchased from Jackson Laboratory, Maine, USA. Mice were housed in the research animal facility at the School of Pharmacy, University of Wyoming, and used for experiments as per approved IACUC protocols. TRPV1^{-/-} mice were genotyped using primers specified by Jackson Laboratories three weeks after birth. We performed genotyping to characterize the absence of TRPV1 genotyping primers for *trpv1*^{-/-} mice [cctgtcacaatgctcattg (forward), tcctcatgcacttcaggaaa (reverse), and tggatgtggaatgtgtgcgag (common)]. The agarose image showing the genotyping data is given in Fig. S2. We have thoroughly characterized the lack of TRPV1 in these mice through western blotting and also routinely perform capsaicin-induced pain responses (intraplantar injections) to analyze nociceptive behaviors. Our westerns and quantitative RT-PCR

experiments that characterized the lack of TRPV1 in these KO mice and the presence of TRPV1 in the wild-type mice were published earlier [3,12].

For experiments, groups of WT and TRPV1^{-/-} mice were fed a normal chow diet (NCD) until six weeks of age and then fed ad libitum either NCD (Labdiet Rodent 5001; gross energy kcal per g is 4.07) or switched to a high-fat diet (HFD; 60% calories from fat; D 12492; Research Diet Inc., New Brunswick, NJ, USA; 5.21 kcal·g⁻¹) until 38 weeks of age. Mice were randomly assigned into feeding groups and were housed in groups of four in separate cages. Mice were maintained in twelve-hr. dark–light cycle, and their weekly weight gain and food and water intake were recorded in a blinded fashion. For energy/water intake, the average quantity consumed per mouse per day was calculated and the mean values of data pooled from week 6 through week 38 of feeding. At the end of 32 weeks of feeding (mice were 38 weeks of age), a metabolic study was performed with a group of mice. Two days after the completion of the metabolic study, epididymal and brown adipose fat pad tissues (EF and BF, respectively) were isolated and used for quantitative RT-PCR experiments.

Metabolic activity measurement

Metabolic activity and respiratory quotient were determined for NCD or HFD-fed WT and TRPV1^{-/-} mice at the end of 32 weeks of feeding by using the Comprehensive Laboratory Animal Monitoring System (CLAMSTM, Columbus Instruments, Columbus, OH, USA) [16,17]. Mice were individually placed in the CLAMS metabolic cages with *ad libitum* access to food and water. After acclimatization for 48 h, metabolic parameters including the volume of carbon dioxide produced (VCO₂), the volume of oxygen consumed (VO₂), the respiratory exchange ratio (RER = VCO₂/VO₂), and ambulatory/locomotor activity were determined as described previously.

Fat tissue isolation [18]

Following euthanization, NCD or HFD-fed WT and TRPV1^{-/-} mice were placed on a surgical pad with dorsal surface up and cut opened along the back to the neck. The intrascapular BF found right under the skin between the shoulders, seen as two lobes, was dissected.

For the SCF isolation, a 1 cm cut through the skin was made using a scalpel just below the rib cage across the dorsal surface joining the two lateral incisions. The skin was peeled, and the fat underlying the muscle and fascia was dissected carefully using a pair of scissors.

Retroperitoneal fat is located in a paravertebral position, along the border between the posterior abdominal wall and the spinal cord. Forceps were used to lift the kidney up and toward the midline to locate the retroperitoneal depots, and the fat was detected.

Gonadal fat is the WAT that surrounds the epididymis and testis in the males and the uterus and ovaries in females. The fat was carefully cut and isolated from the NCD or HFD-fed male and female WT and TRPV1^{-/-} mice.

Following the isolation of fat pads, organs were carefully isolated and weighed. The weights of the fat pads and organs were determined and represented in Fig. S1.

Adipose histology

After euthanization, the adipose fats (epididymal and brown) were isolated and quickly fixed in 10% formalin solution. Fixed tissues were processed through graded ethanol solutions, transferred to xylene, and then embedded in paraffin. The paraffinized tissues were then sectioned at 8 μ m thickness and mounted on glass slides. The sections were then deparaffinized through xylene followed by ethanol. Finally, the hydrated sections were stained with hematoxylin and eosin and then coverslipped using permount. Sections were examined microscopically.

Quantitative RT-PCR measurements

Total RNA was isolated using Tri-reagent (Sigma, St. Louis, MO, USA) as per the manufacturer's instructions. cDNA was synthesized using QuantiTect reverse transcription kit (Qiagen, Valencia, CA, USA) using Q5plex PCR system (Qiagen). Real-time PCR was performed using QuantiTect SYBR Green PCR kit on the Q5plex system. 18s mRNA was used as the internal control. The scientist who performed these experiments was blinded by the type of tissues processed for these experiments. Amplifications were performed in a 25- μ L-reaction volume. Primers used for quantitative RT-PCR experiments are given in Table 1.

Immunoblotting

Isolated fat pads were washed with chilled PBS, lysed in lysis buffer (50 mM Tris pH 7.5, 250 mM sodium chloride, 0.5% NP-40, 0.5% sodium deoxycholate, 2 mM EDTA, 0.5 mM dithiothreitol, 1 mM sodium orthovanadate, and protease inhibitor cocktail), and centrifuged at 20 817 g for

20 min. to remove tissue debris. The concentration of protein was determined by the Bradford method, and equal amounts of protein were separated by SDS/PAGE, transferred to a nitrocellulose membrane, and immunoblotted with antibodies given in Table 2.

Blood glucose and cholesterol measurement

Mice were fasted for 6 h before measuring blood glucose and cholesterol measurement. Blood glucose was measured by using a glucometer (Counter Next monitoring system and strips, Bayer, Pittsburgh, PA, USA). Fasting serum cholesterol level was measured using a commercially available kit (BioVision, Milpitas, CA, USA).

Intraperitoneal glucose tolerance test [12]

IPGTT was performed after fasting mice for 8 h. Mice were injected with glucose (2 g·kg⁻¹) intraperitoneally. Blood glucose was measured, via tail vein bleeding, with a glucometer at 0, 15, 30, 60, and 120 min. Briefly, the mouse was made comfortable in a restrainer while maintaining the temperature around 27–28 °C on a thermal blanket. A 25 G needle was inserted into the blood vessel, and blood is collected using a capillary tube. After blood collection, bleeding was stopped by applying pressure using a sterile gauze pad.

Determination of plasma glucagon-like peptide-1 (GLP-1) level

Following fasting for 8 h, mice were fed food *ad libitum* for 2 h and blood was drawn into EDTA tubes (BD Biosciences, San Jose, CA, USA) containing 10 mL of DPP-IV inhibitor (Millipore, Burlington, MA, USA) at 10 PM. The tubes were inverted, mixed well, and centrifuged at 1000 g for 10 min. in a refrigerated centrifuge. GLP-1 in plasma samples was determined as per the manufacturer's instruction (Alpco, Salem, NH, USA) using a TECAN plate reader.

Table 1. Quantitative RT-PCR Primers used in the study.

Gene	Forward (5'-3')	Reverse (5'-3')
18s	accgcagctaggaataatgga	gcctcagttccgaaaacca
<i>mtrpv1</i>	caacaagaaggggttacc	tctggagaatgtaggccaagac
<i>pparα</i>	gtaccactacggagttcagcat	cgccgaaagaagcccttac
<i>pparγ</i>	aagaataccaaagtgcgatcaa	gagcagggtctttcagaataataag
<i>sirt1</i>	tcgtggagacatttttaacagg	gcttcgatggaagcagtg
<i>Prdm16</i>	cagcacggggaagccattc	gcgtgatccgctgtg
<i>bmp8b</i>	tccaccaaccagccactat	cagtaggcacacagcacct
<i>Ucp1</i>	cgactcagccaagagtactctcttc	gccggctgagatctgtttc
<i>pgc1α</i>	agagagcagaagcagaagaacat	attctgtccgctgtgtcagg

Table 2. Antibodies used in the study.

Protein	Catalog number	Source
GAPDH	2118	Cell Signaling Technologies, Inc., Danvers, MA, USA
PPAR α	NB600-636	Novus Biologicals, Centennial, CO, USA
PPAR γ	SC-7273	Santa Cruz Biotechnology, Inc., Dallas, TX, USA
SiRT-1	SC-28766	Santa Cruz Biotechnology, Inc.
PRDM-16	NBP1-77096	Novus Biologicals
UCP-1	14670	Cell Signaling Technologies, Inc.
PGC-1 α	ab54481	Abcam, Cambridge, MA, USA

Oil red O staining of liver sections

Six to ten mm OCT liver sections from NCD or HFD-fed WT and TRPV1^{-/-} mice were fixed in formalin, washed three times with PBS, and then rinsed in 60% isopropyl alcohol for 2 min followed by Oil Red O (ORO) in polyethylene glycol for 15 min. The sections were then rinsed with water, and the nucleus was stained with hematoxylin for 10 min. The nuclear staining was intensified with sodium phosphate solution for 5 min, washed with water several times, and mounted using an aqueous mounting medium. The sections were then visualized under a Zeiss 700 confocal microscope.

Liver histology sections

At the end of feeding NCD or HFD, WT and TRPV1^{-/-} mice were euthanized as per approved IACUC protocol. Liver tissue was isolated and fixed in 10% formalin solution. Fixed liver tissues were processed, using routine procedures, through graded ethanol solutions, into xylene then were embedded in paraffin. The paraffinized liver tissues were then sectioned at 8 microns, mounted onto glass slides, then deparaffinized through xylene then ethanol solutions. The hydrated sections were finally stained with hematoxylin and eosin before a final step of dehydration then coverslipped using permount®.

Drugs and chemicals

All special diets were obtained from Research Diets Inc., New Brunswick, NJ, USA. All chemicals are obtained from Sigma. Quantitative RT-PCR kits were obtained from Qiagen, USA.

Statistical analyses

Data for all figures were expressed as mean ± SEM. Student *t*-test and ANOVA evaluated the statistical significance of population means. Samples sizes were set to determine whether the mean value of an outcome variable in one group differed significantly from that in another group. A *P* value < 0.05 was considered statistically significant. Figures from analyzed data were plotted using MICRO-CAL ORIGIN 2020 software (OriginLab Corporation, Northampton, MA, USA).

Results

To determine whether lack of TRPV1 protects against HFD-induced obesity, we fed TRPV1^{-/-} mice either NCD or HFD. WT mice fed with these diets were used as controls. As shown in Fig. 1A, HFD feeding caused significant weight gain in both WT and TRPV1^{-/-} mice. HFD feeding caused an increase in

the bodyweight of TRPV1^{-/-} mice in the weeks of 10–15 and 25–30. However, at 32 weeks of feeding HFD, we did not observe any significant difference in the body weight of WT and TRPV1^{-/-} mice. Further, NCD-fed TRPV1^{-/-} mice also gained slightly but significantly higher weight compared with WT. But the quantity of food (energy intake) or water consumed by these groups of mice (Fig. 1B,C) did not differ from the WT. Also, consistent with the gain in body weight due to HFD feeding, organ weights and fat mass were higher for the HFD-fed groups compared with NCD-fed mice (Fig. S1). Next, we performed a histology section of white and brown fat to evaluate the size of eWAT and BAT of NCD or HFD-fed WT and TRPV1^{-/-} mice. As illustrated in Fig. 1D,E, adipose hypertrophy was observed in HFD-fed groups.

We evaluated the effect of HFD feeding on the VCO₂, VO₂, respiratory exchange ratio (RER = VCO₂/VO₂), and energy utilization by indirect calorimetry. We also measured the locomotor activity in these mice. These data are given in Fig. 1F through R. We did not observe any difference in the RER as HFD suppressed RER to a similar extent in both groups. But the energy utilization and locomotor activity (in the dark cycle) were significantly less in NCD-fed TRPV1^{-/-} mice compared with WT.

Since HFD significantly caused obesity in both WT and TRPV1^{-/-} mice, we analyzed whether the expression of adipogenic and thermogenic genes is similarly downregulated by HFD in both groups. For this, we isolated epididymal fat (white fat) and intrascapular brown fat and quantified the expression of adipogenic and thermogenic genes by quantitative RT-PCR technique. We first evaluated the expression of TRPV1 in NCD and HFD-fed WT and TRPV1^{-/-} mice. As shown in Fig. 2A,B, TRPV1 was expressed in both EF and BF of WT but not in TRPV1^{-/-} mice. However, HFD significantly suppressed TRPV1 mRNA in both EF and BF.

Next, we analyzed the mRNA levels of peroxisome proliferator activator receptor (PPAR) alpha (PPAR α) and PPAR γ in the EF and BF of these mice. As shown in Fig. 2C, both PPAR α and PPAR γ mRNA levels were lower in EF of NCD-fed TRPV1^{-/-} mice compared with WT. However, PPAR γ mRNA was elevated in the BF of HFD-fed WT and TRPV1^{-/-} mice. Also, HFD did not reduce PPAR α in the BF of WT but suppressed in the BF of TRPV1^{-/-} mice.

Next, we evaluated the mRNA levels of thermogenic mitochondrial UCP-1 and BMP8b, which take part in thermogenesis. In the EF of NCD-fed TRPV1^{-/-} mice, the UCP-1 level was significantly less compared with WT. Consistently, NCD-fed TRPV1^{-/-} mice

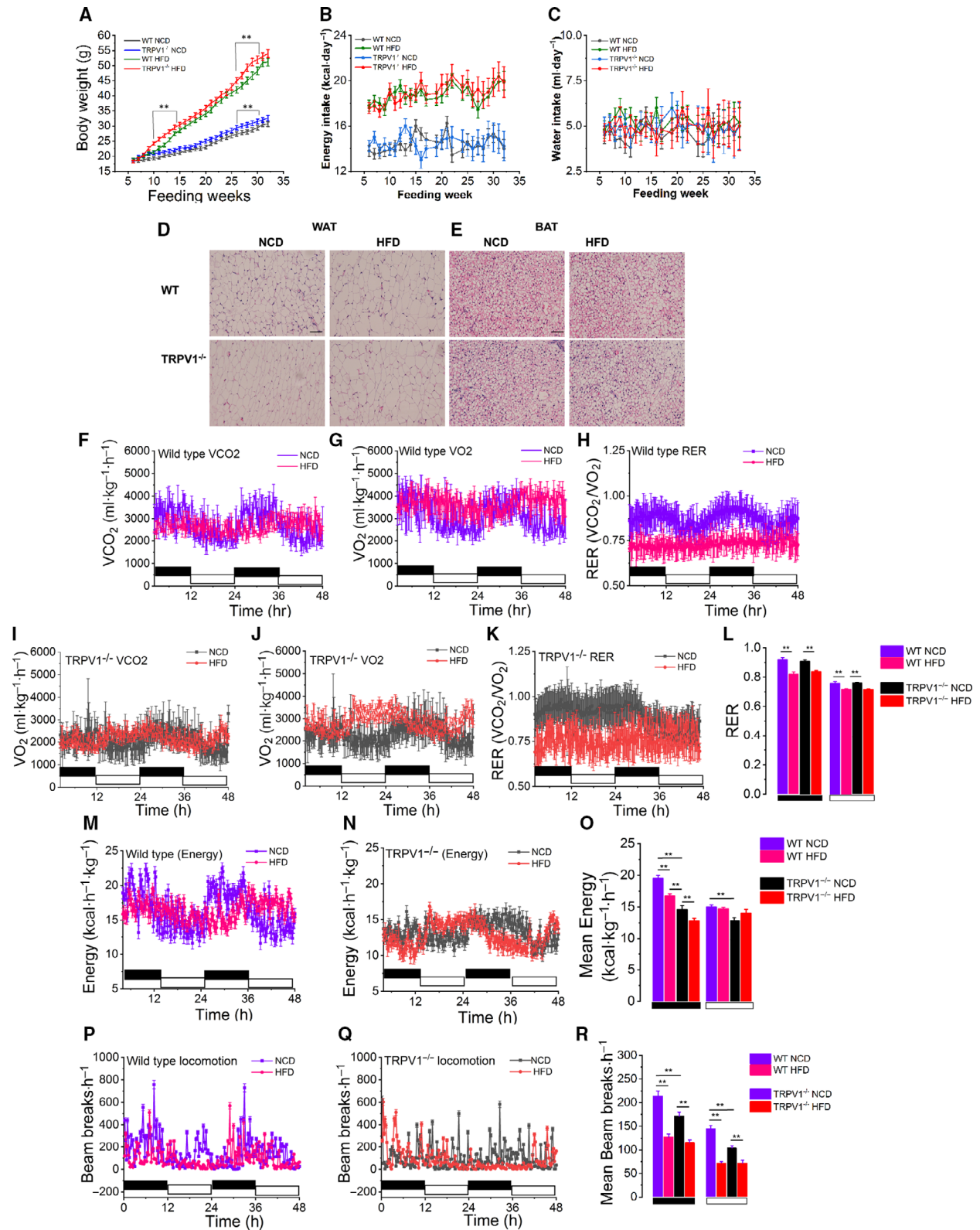
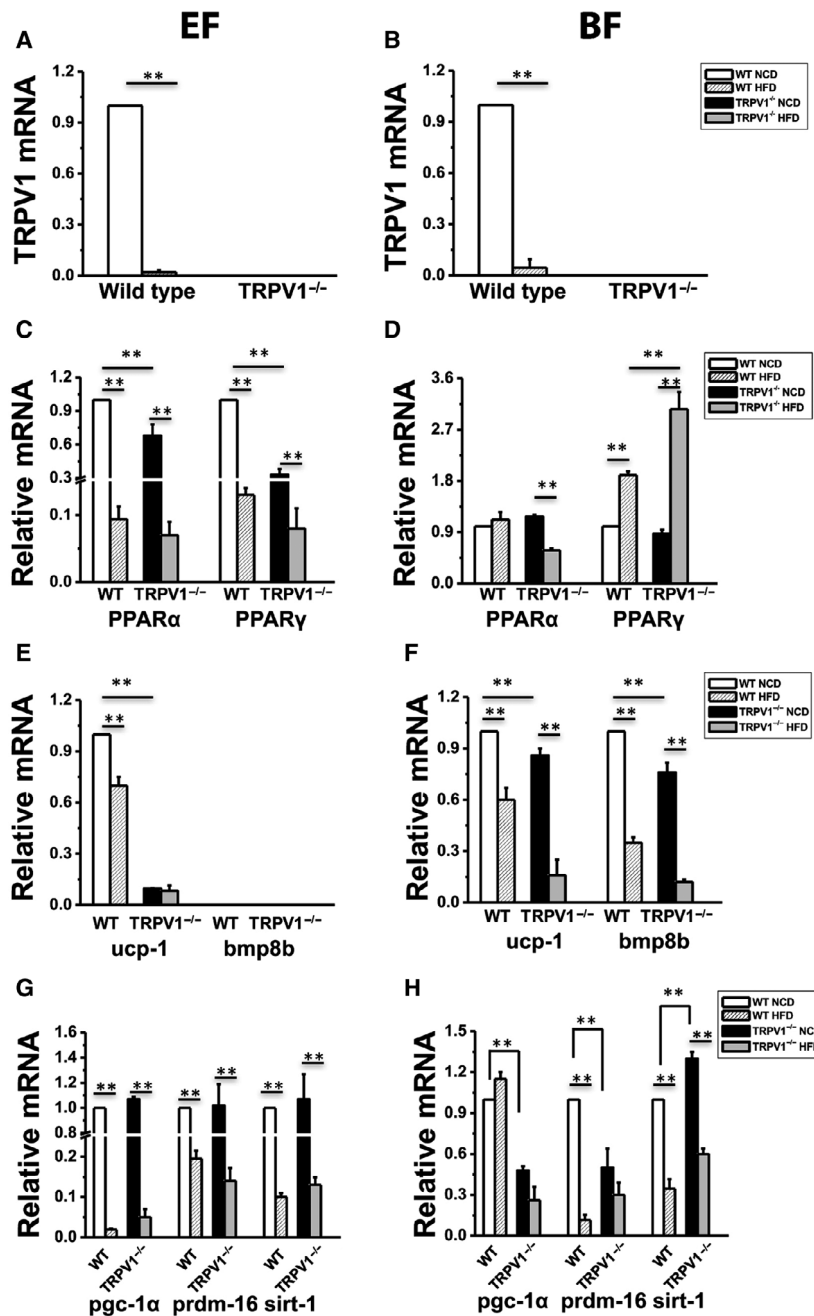


Fig. 1. Effects of NCD and HFD feeding on weight gain, food/water intake, metabolic, and locomotor activities in NCD or HFD-fed WT and TRPV1^{-/-} mice. (A) Time courses of body weight gain (g) ± SEM in NCD or HFD-fed WT and TRPV1^{-/-} mice. (B, C) Mean energy/water intake ± SEM intake per day in these mice. (D, E) Hematoxylin and Eosin staining for epididymal white (D) and brown (E) fats of WT and TRPV1^{-/-} mice. Time courses of VCO₂, VO₂, and RER in the dark and light cycle (black and white boxes, respectively) for WT (F–H) and TRPV1^{-/-} (I–K) mice at the end of 32 weeks of feeding NCD or HFD. (L) Mean RER ± SEM for these mice. Time courses of energy expenditure in the dark and light cycle for WT (M) and TRPV1^{-/-} (N) mice. (O) Mean energy expenditure ± SEM for these mice. Time courses of locomotor activity in the dark and light cycle for WT (P) and TRPV1^{-/-} (Q) mice. (R) Mean locomotor activity ± SEM for these mice. **Statistical significance at *P* < 0.05 for *n* = 12 per condition.



expressed significantly lower levels of UCP-1 and BMP8b in the BF. Neither NCD nor HFD-fed WT and TRPV1^{-/-} mice had BMP8b mRNA in the EF. HFD feeding inhibited the mRNA level of UCP-1 and BMP8b in the BF in both WT and TRPV1^{-/-} mice.

We measured the mRNA levels of genes that regulate the browning of WAT and BAT thermogenesis. We analyzed the mRNA level of SiRT-1, an NAD⁺-dependent deacetylase. SiRT-1 triggers browning of WAT by deacetylating PPAR γ and PRDM-16 and facilitating their interaction. PRDM-16 is a transcription factor that promotes browning of WAT and PPAR γ coactivator 1 α (PGC-1 α) regulates mitochondrial biogenesis, UCP-1 transcription, and brown fat activation [19]. The mRNA levels of these genes are given in Fig. 2G,H. Although we did not observe any difference in the levels of SiRT-1, PRDM-16, and PGC-1 α in the EF of WT and TRPV1^{-/-} mice (Fig. 2G), they were significantly reduced in the BF of NCD-fed TRPV1^{-/-} mice (Fig. 2H). The mRNA of SiRT-1, PRDM-16, and PGC-1 α in both EF and BF of WT and TRPV1^{-/-} mice was decreased under HFD-fed conditions. Further, it is interesting to note that SiRT-1 mRNA was enhanced in the NCD-fed TRPV1^{-/-} mice compared with WT.

Next, we evaluated the expression of thermogenic proteins in the BF and SCF isolated from these mice. Immunoblotting experiments demonstrated that the endogenous expression of PPAR α , PPAR γ , PGC-1 α , PRDM-16, SiRT-1, UCP-1, and was higher in the WT compared with TRPV1^{-/-} mice in the BAT (Fig. 3). Also, the expression of all these proteins was suppressed in HFD-fed WT and TRPV1^{-/-} mice. The enhancement of PPAR γ mRNA in the BF of TRPV1^{-/-} mice (Fig. 2D) did not correlate with the protein expression in the BAT of these mice (Fig. 3B). Similar to BF, HFD feeding for 32 weeks suppressed the expression of thermogenic proteins in the inguinal WAT of WT and TRPV1^{-/-} mice (Fig. 4).

HFD-induced obesity is often associated with fatty liver. Since TRPV1 is implicated in fatty liver disease, we analyzed whether TRPV1^{-/-} is protected from a fatty liver caused by feeding HFD. As shown in Fig. 5A through C, HFD feeding resulted in hepatic steatosis and fat accumulation in the liver of both WT and TRPV1^{-/-} mice. Also, the steatosis score and ballooning calculated by the method explained by Kleiner *et al.* [20] were higher in the liver sections

of TRPV1^{-/-} mice compared with WT mice. However, hepatic steatosis is more pronounced in the liver of TRPV1^{-/-} mice.

Next, we measured IPGTT and postfeeding plasma GLP-1 levels in NCD or HFD-fed WT and TRPV1^{-/-} mice. HFD feeding resulted in hyperglycemia (Fig. 6A), hypercholesterolemia (Fig. 6B), and inhibited plasma GLP-1 levels (Fig. 6C). Also, HFD feeding caused glucose intolerance (Fig. 6D,E) in both WT and TRPV1^{-/-} mice.

Discussion

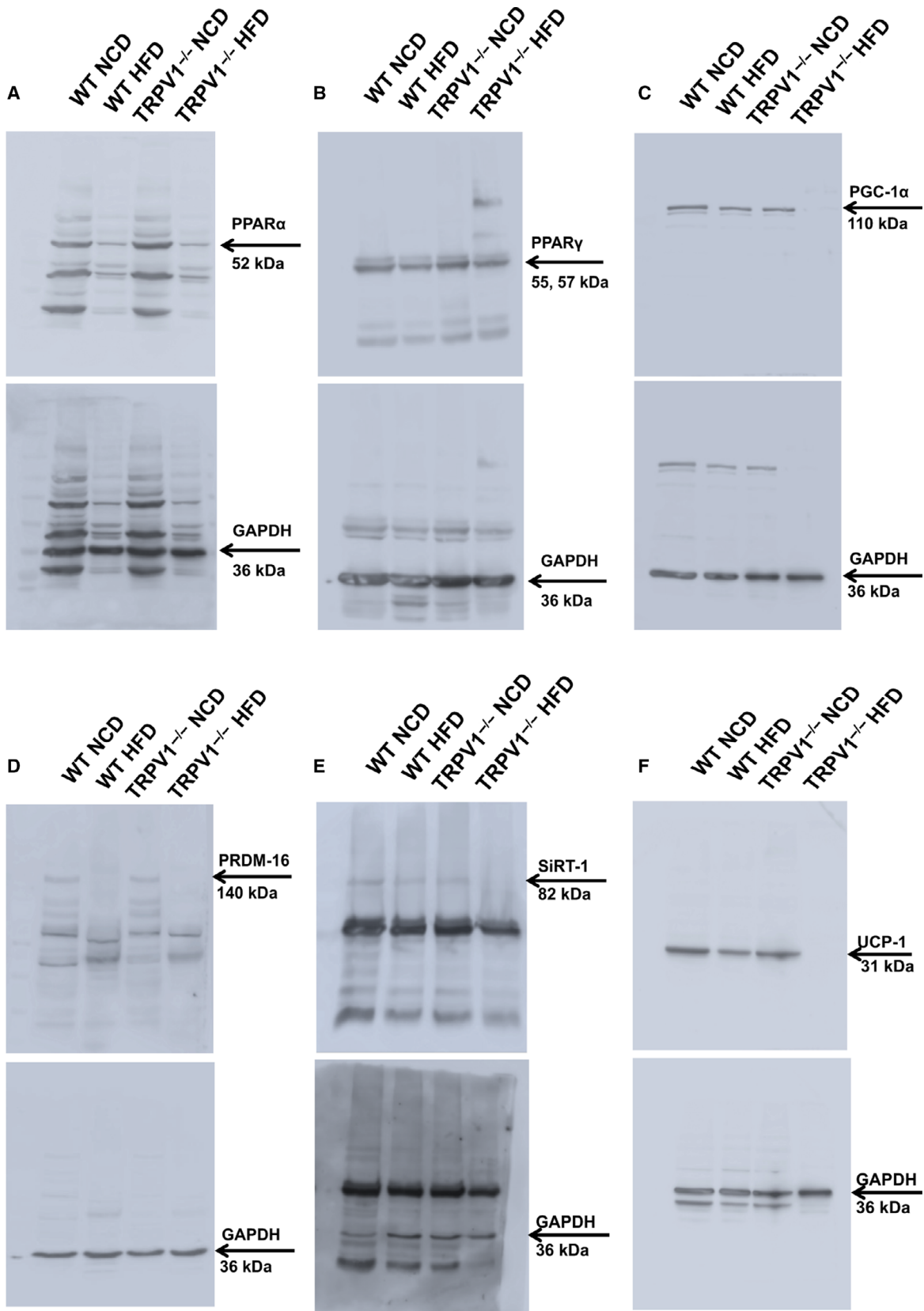
Obesity leads to metabolic dysfunction. Currently, two billion people in the world are overweight and one third are obese [21]. Recent research suggests that TRPV1 is an emerging target for obesity management [4,6,8–10,13]. However, studies also indicate that lack of TRPV1 protects against obesity and metabolic complications [9,13,14]. The primary focus of this study is to resolve this controversy by evaluating whether TRPV1^{-/-} mice were resistant to HFD-induced obesity.

Our data demonstrate that HFD feeding caused an increase in body weight in both WT and TRPV1^{-/-} mice. Interestingly, TRPV1^{-/-} mice gained significantly more weight during the weeks 10–15 and 25–30, compared with wild-type mice, without a concomitant change in energy intake (Fig. 1A–C). Thus, TRPV1^{-/-} mice were not resistant to HFD-induced obesity. This observation is in contrast with a previous work suggesting that lack of TRPV1 protected mice from diet-induced obesity [9]. One reason for this discrepancy is the type of HFD and the amount of fat from calories in these studies. The number of calories from fat was observed to be 25.8% in the Purina Diet 5015 used by Motter and Ahern, 2008 [9], while 60% in this and previous studies [3,22].

Also, the weights of inguinal, retroperitoneal, and gonadal fats were significantly increased in the HFD-fed mice in both groups, the draw weights of both inguinal and retroperitoneal WAT higher in HFD-fed TRPV1^{-/-} mice compared with WT. Adipose hypertrophy was observed in both groups of mice-fed HFD compared with NCD-fed conditions.

Analysis of metabolic activity studies revealed that NCD-fed TRPV1^{-/-} mice exhibited less energy expenditure (Fig. 1M–O) and reduced locomotor activity (Fig. 1P–R). Energy expenditure was more

Fig. 3. Adipogenic and thermogenic protein expression in the intrascapular BAT of NCD or HFD-fed WT and TRPV1^{-/-} mice. Representative western blot showing the expression of PPAR α (A) and PPAR γ (B), PGC-1 α (C), PRDM-16 (D), SiRT-1 (E), and UCP-1 (F) in the intrascapular BAT of NCD or HFD-fed WT and TRPV1^{-/-} mice.



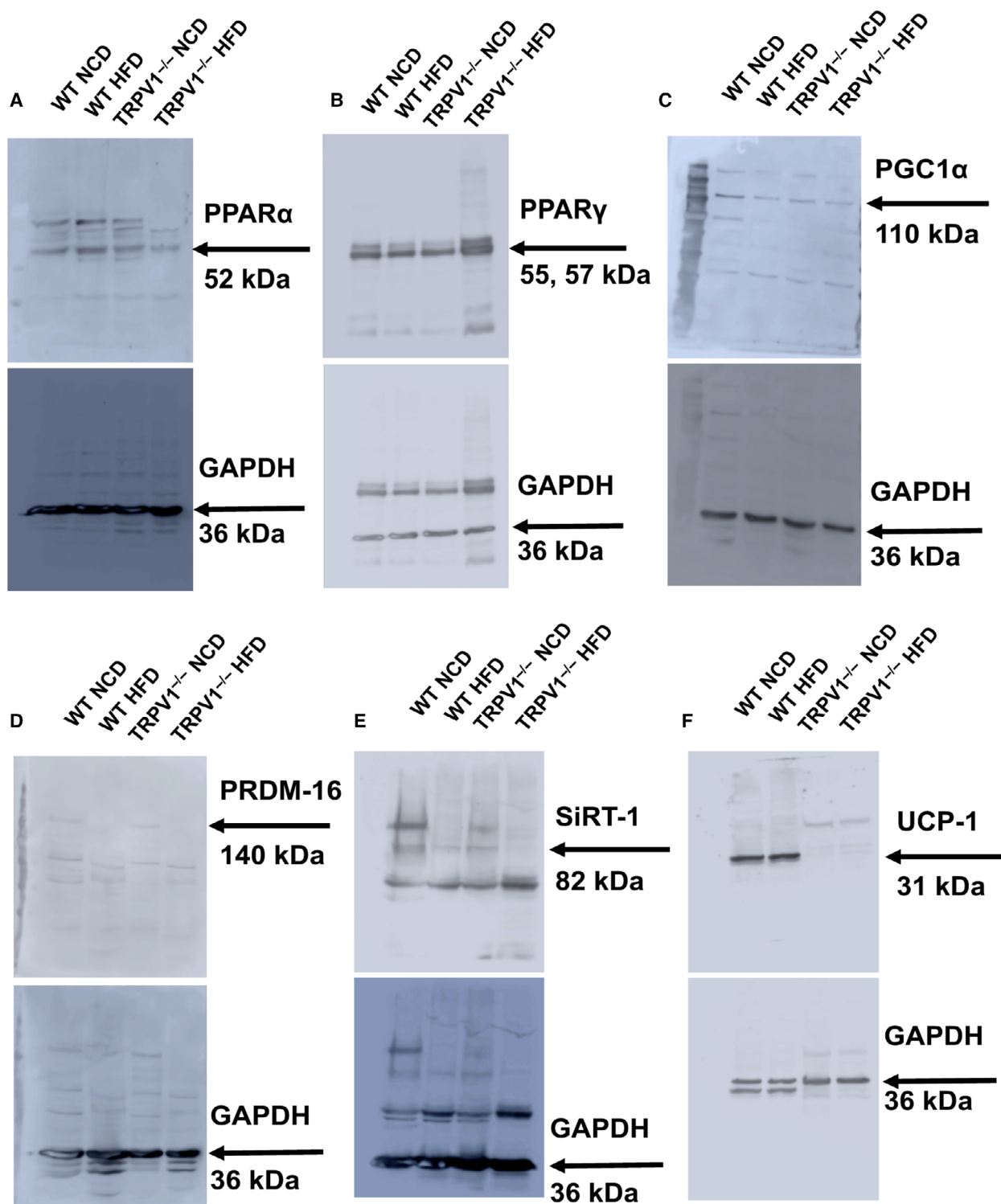


Fig. 4. Adipogenic and thermogenic protein expression in the subcutaneous (inguinal) WAT of NCD or HFD-fed WT and TRPV1^{-/-} mice. Representative western blot showing the expression of PPAR α (A) and PPAR γ (B), PGC-1 α (C), PRDM-16 (D), SiRT-1 (E), and UCP-1 (F) in the inguinal WAT of NCD or HFD-fed WT and TRPV1^{-/-} mice.

Fig. 5. HFD-induced fatty liver is enhanced in TRPV1^{-/-} mice. (A) Hematoxylin and eosin staining showing hepatic steatosis in NCD or HFD-fed WT (top panel) and TRPV1^{-/-} (bottom panel) mice (*n* = 6 per condition). (B) Oil red O staining in the liver sections of WT (top panel) and TRPV1^{-/-} mice (bottom panel) (*n* = 6 per condition). (C) Steatosis and ballooning scores for the liver sections of WT and TRPV1^{-/-} mice. Scale bar represents 50 μm. **Statistical significance at *P* < 0.05 for *n* = 5 per condition.

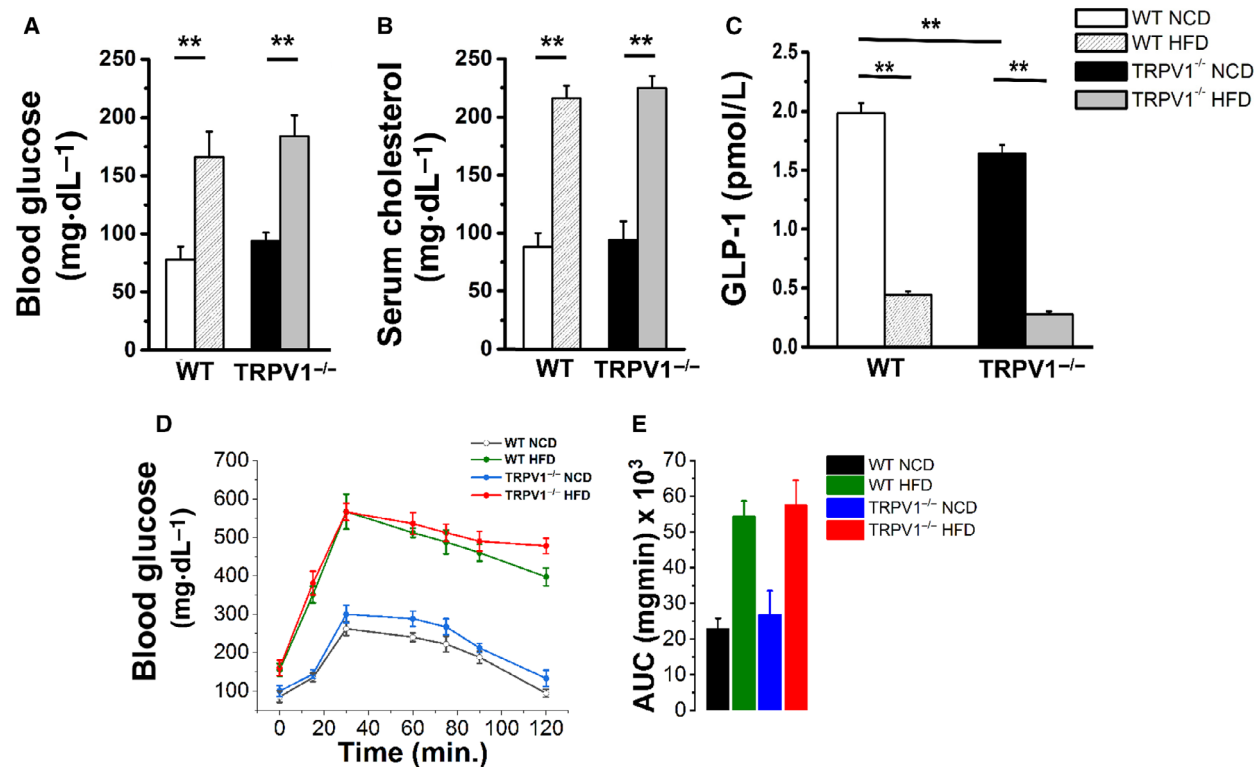
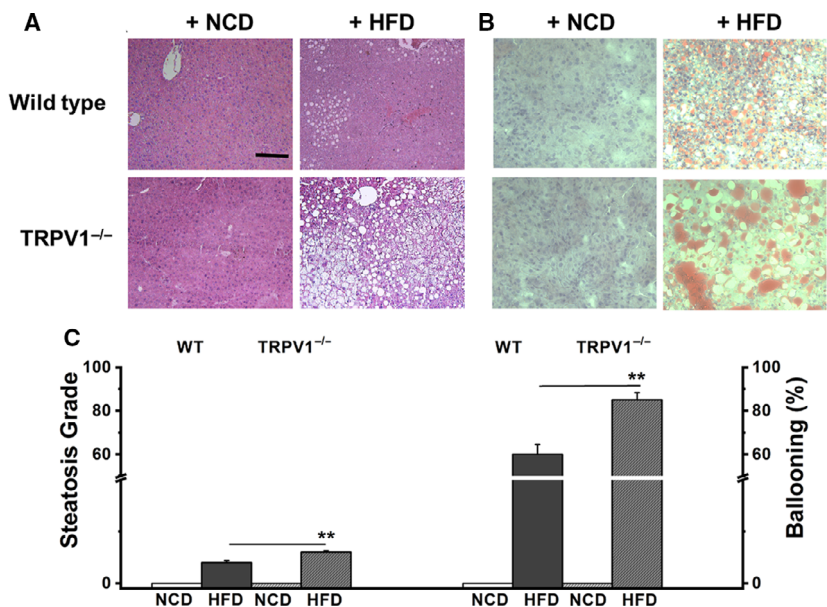


Fig. 6. HFD feeding impairs glucose handling and causes glucose intolerance and hypercholesterolemia in WT and TRPV1^{-/-} mice. Mean fasting blood glucose ± SEM (A; *n* = 6) mean fasting serum cholesterol ± SEM (B; *n* = 6) and mean plasma GLP-1 ± SEM (C; *n* = 6) in the WT and TRPV1^{-/-} mice at the end of 32 weeks of feeding NCD or HFD. D. IPGTT in WT and TRPV1^{-/-} mice (*n* = 6). E. The area under the curve ± SEM for these mice. **Statistical significance at *P* < 0.05 for *n* = 6 per condition.

significantly decreased in the active dark cycle of NCD-fed TRPV1^{-/-} mice, while locomotor activity was reduced in both dark and light cycles compared

with WT. These may contribute to the slight but significant weight gain observed in the TRPV1^{-/-} mice. In contrast to this observation, previous research

showed that TRPV1^{-/-} mice exhibited higher locomotor and basal hypometabolic (lower oxygen consumption) activities at 27 °C [23]. This can be due to the differences in the experimental conditions as our studies were performed at 22–24 °C and not at 27 °C. Another possible reason could be the age of the mice used in the experiments. That is, previous research showed that older TRPV1^{-/-} mice showed reduced locomotor activity compared with younger ones [24]. Our experiments were performed with 38-week-old mice, and under these conditions, TRPV1^{-/-} mice showed reduced locomotor activity in both light and dark cycles. But, in HFD-fed obese mice, locomotor activity was reduced in both groups.

One limitation of the current study is that it compared the locomotor activities of 38-week-old WT and TRPV1^{-/-} mice-fed NCD or HFD. The contribution of the age of the mice has to be weighed in, and future studies are required to analyze the effect of aging on metabolic and locomotor activities in the WT and TRPV1^{-/-} mice. Nonetheless, these data clarify that TRPV1 is implicated in locomotor activity regulation but how TRPV1 regulates locomotor activity remains to be resolved.

The reduced locomotor activity observed in NCD-fed TRPV1^{-/-} mice can be due to neurological changes. For example, the reduction in SiRT-1 in TRPV1^{-/-} mice may cause these changes presumably due to an overall reduction in metabolism. But it is difficult to correlate the reduction in SiRT-1 in adipose tissues to affect locomotor behaviors. Nonetheless, an overall reduction in the locomotor activity associated with reduced energy expenditure in the dark and light cycles may lead to an increase in body weight of NCD-fed TRPV1^{-/-} mice.

Interestingly, TRPV1 inhibitors are shown to increase energy metabolism [25–27]. However, in the physiological context, the lack of expression of TRPV1 does not mimic the inhibition of TRPV1 activity. Moreover, TRPV1 inhibitors are known to cause hyperthermia in WT mice, which is an undesired side effect of such compounds [28,29]. Further studies using thermoneutral TRPV1 inhibitors [30] are required to clarify the role of TRPV1 in the regulation of metabolic activity. Also, several of these studies have evaluated metabolic activity only acutely in TRPV1^{-/-} mice, while the results presented in this study were conducted for 48 h after 32 weeks of feeding NCD or HFD.

Previous research demonstrates the involvement of TRPV1 in the transcription regulatory process in thermal regulation and inflammation [31,32]. In this study, we observed a significant difference between the expression levels of adipogenic and thermogenic transcription

factors in the white and brown fat of NCD or HFD-fed WT and TRPV1^{-/-} mice (Fig. 2). These transcription factors regulate adipogenesis, adipocyte maturation [33], and fatty acid metabolism [34,35]. Also, we observed that TRPV1^{-/-} mice expressed reduced thermogenic proteins compared with WT endogenously (Figs 3 and 4). This is a striking observation but the mechanism by which TRPV1 regulates the expression of transcription factors, which govern adipogenic and thermogenic mechanisms, remains to be resolved. The reduced expression of UCP-1 in the TRPV1^{-/-} correlates with the decrease in PPAR α since PPAR α regulates the transcription of UCP-1 [36]. Also, HFD feeding suppressed both PPAR α and UCP-1 in EF.

In contrast to EF, we did not see a significant difference in the mRNA of PPARs in the BF of WT and TRPV1^{-/-} NCD-fed mice. However, the levels of UCP-1 and BMP8b were both decreased in the TRPV1^{-/-} mice. Similarly, the levels of PRDM16 and PGC-1 α , which regulate BF differentiation and activation respectively, are decreased in BF. Taken together, this indicates that a deficit in the thermogenic machinery in the BF of TRPV1^{-/-} mice could make them more susceptible to metabolic dysfunctions when challenged with HFD. Surprisingly, we found an increase in the expression level of sirtuin 1 mRNA in NCD-fed TRPV1^{-/-} mice compared with WT mice. However, the SiRT-1 protein expression was reduced in these mice, even under NCD-fed conditions.

It is important to note that the mRNA and protein levels of adipogenic and thermogenic markers in the NCD or HFD-fed WT and TRPV1^{-/-} mice lack a stoichiometric correlation. Therefore, a careful interpretation is necessary for determining the specific effect of a decrease or increase in mRNA and protein levels in research studies. However, based on the analysis of protein expression, NCD-fed TRPV1^{-/-} mice expressed lower levels of adipogenic and thermogenic proteins in the SCF and BF, except PRDM-16 in the SCF. This could be a reason for the higher weight gain observed in the TRPV1^{-/-} mice.

Further, this research presents another important observation that TRPV1 was downregulated by HFD feeding in the WT mice. Lipid accumulation in 3T3-L1 adipocytes has previously been shown to inhibit TRPV1 [11]. But the mechanism behind this remains to be determined. A possible mechanism may include the suppression of transcriptional factors that regulate TRPV1 expression by HFD [37]. This has to be further evaluated to clarify the mechanism by which HFD suppresses TRPV1. Moreover, it is important to note that chronic HFD feeding downregulated the expression of several thermogenic proteins.

Fatty liver is a common comorbidity associated with obesity [38,39]. Fatty liver also occurs independently of obesity [40]. Our data indicate that fatty liver occurred in both WT and TRPV1^{-/-} mice that received HFD. Further, the intensity of hepatic steatosis was seen more pronounced in the TRPV1^{-/-} mice, as evidenced by higher steatosis scores and hepatic ballooning (Fig. 5A,B). This observation raises an important question—what is the physiological role of TRPV1 in the regulation of lipid metabolism in the liver? PPAR α is important for lipid metabolism, and there was a reduction in endogenous PPAR α protein expression in TRPV1^{-/-} mice. Therefore, it is reasonable to speculate that the reduced expression of PPAR α in HFD-fed WT and TRPV1^{-/-} mice decreases fatty acid oxidation in the liver of these mice. This could cause impairment of glucose handling in these mice. These effects associated with a reduction in GLP-1 levels in these mice may underlie the cause of metabolic dysfunctions in these mice.

Overall, our data indicate that the lack of TRPV1 does not protect mice from diet-induced obesity. Further, endogenous TRPV1 regulates the expression of adipogenic transcriptional factors (PPARs) and thermogenic genes and proteins in EF, SCF, and BF of TRPV1^{-/-} mice. Given its role in adipocyte differentiation, browning of WAT and BAT thermogenesis, the implication of TRPV1 in metabolic regulation cannot be ignored. Our data also suggest that TRPV1^{-/-} mice could be more susceptible to metabolic dysfunction due to decreased expression of thermogenic genes in the white and brown fat. The increased steatosis was seen in TRPV1^{-/-} mice, following HFD-mediated metabolic insult (Fig. 5), which also suggests that a lack of TRPV1 may play a role in basal lipid metabolism. But the mechanism behind this remains unclear. Consistent with this, a previous report suggests that NCD-fed TRPV1^{-/-} mice had a higher random blood glucose level compared with WT mice [14]. However, the precise effects of lack of TRPV1 in neurological and adipose tissue-dependent functions remain to be determined. Nonetheless, our work clarifies that lack of TRPV1 does not protect mice from obesity but rather exacerbates HFD-induced metabolic dysfunction. TRPV1^{-/-} mice exhibit decreased expression of thermogenic proteins in white and brown fats, which is suggestive of a significant genotypic difference between them and WT mice.

Acknowledgements

This work was supported by funding from a pilot project of the National Institute of General Medical

Sciences of the NIH under award number 8P20 GM103432-12 and WY NASA Faculty Research Initiation Grant for BT.

Author contributions

PB performed qRT-PCR, immunoblotting, and ELISA experiments, analyzed results, and wrote the manuscript. KN, JF, and JO maintained animals recorded weight gain, food/energy, and water intake, helped with western blotting, and performed metabolic activity experiments. BT conceived the concept, designed experiments, performed experiments, analyzed results, and wrote the manuscript.

Data accessibility

Data supporting the findings are available in the figures, tables, and supplementary material of this article.

References

- Luo Z, Ma L, Zhao Z, He H, Yang D, Feng X, Ma S, Chen X, Zhu T, Cao T *et al.* (2012) TRPV1 activation improves exercise endurance and energy metabolism through PGC-1 α upregulation in mice. *Cell Res* **22**, 551–564.
- Li L, Chen J, Ni Y, Feng X, Zhao Z, Wang P, Sun J, Yu H, Yan Z, Liu D *et al.* (2012) TRPV1 activation prevents nonalcoholic fatty liver through UCP2 upregulation in mice. *Pflugers Arch* **463**, 727–732.
- Baskaran P, Krishnan V, Ren J and Thyagarajan B (2016) Capsaicin induces browning of white adipose tissue and counters obesity by activating TRPV1 channel-dependent mechanisms. *Br J Pharmacol* **173**, 2369–2389.
- Zhang LL, Yan Liu D, Ma LQ, Luo ZD, Cao TB, Zhong J, Yan ZC, Wang LJ, Zhao ZG, Zhu SJ *et al.* (2007) Activation of transient receptor potential vanilloid type-1 channel prevents adipogenesis and obesity. *Circ Res* **100**, 1063–1070.
- Yoneshiro T, Aita S, Kawai Y, Iwanaga T and Saito M (2012) Nonpungent capsaicin analogs (capsinoids) increase energy expenditure through the activation of brown adipose tissue in humans. *Am J Clin Nutr* **95**, 845–850.
- Chen J, Li L, Li Y, Liang X, Sun Q, Yu H, Zhong J, Ni Y, Chen J, Zhao Z *et al.* (2015) Activation of the TRPV1 channel by dietary capsaicin improves visceral fat remodeling through connexin43-mediated Ca²⁺ influx. *Cardiovasc Diabetol* **14**, 22.
- Choowanthanapakorn M, Lu KW, Yang J, Hsieh CL and Lin YW (2015) Targeting TRPV1 for body weight

- control using TRPV1(-/-) mice and electroacupuncture. *Sci Rep* **5**, 17366.
- 8 Lee E, Jung DY, Kim JH, Patel PR, Hu X, Lee Y, Azuma Y, Wang H-F, Tsitsilianos N, Shafiq U *et al.* (2015) Transient receptor potential vanilloid type-1 channel regulates diet-induced obesity, insulin resistance, and leptin resistance. *FASEB J* **29**, 3182–3192.
 - 9 Motter AL and Ahern GP (2008) TRPV1-null mice are protected from diet-induced obesity. *FEBS Lett* **582**, 2257–2262.
 - 10 Yu Q, Wang Y, Yu Y, Li Y, Zhao S, Chen Y, Waqar AB, Fan J and Liu E (2012) Expression of TRPV1 in rabbits and consuming hot pepper affects its body weight. *Mol Biol Rep* **39**, 7583–7589.
 - 11 Krishnan V, Baskaran P and Thyagarajan B (2019) Troglitazone activates TRPV1 and causes deacetylation of PPARgamma in 3T3-L1 cells. *Biochim Biophys Acta Mol Basis Dis* **1865**, 445–453.
 - 12 Baskaran P, Krishnan V, Fettel K, Gao P, Zhu Z, Ren J and Thyagarajan B (2017) TRPV1 activation counters diet-induced obesity through sirtuin-1 activation and PRDM-16 deacetylation in brown adipose tissue. *Int J Obes (Lond)* **41**, 739–749.
 - 13 Marshall NJ, Liang L, Bodkin J, Dessapt-Baradez C, Nandi M, Collot-Teixeira S, Smillie S-J, Lalgı K, Fernandes ES, Gnudi L *et al.* (2013) A role for TRPV1 in influencing the onset of cardiovascular disease in obesity. *Hypertension* **61**, 246–252.
 - 14 Motter A (2011) Doctoral Thesis – Novel Roles for TRPA1 and TRPV1 in Nutrient Sensing and Obesity. Georgetown University, Washington, DC.
 - 15 Baboota RK, Murtaza N, Jagtap S, Singh DP, Karmase A, Kaur J, Bhutani KK, Boparai RK, Premkumar LS, Kondepudi KK *et al.* (2014) Capsaicin-induced transcriptional changes in hypothalamus and alterations in gut microbial count in the high-fat diet fed mice. *J Nutr Biochem* **25**, 893–902.
 - 16 Turdi S, Kandadi MR, Zhao J, Huff AF, Du M and Ren J (2011) Deficiency in AMP-activated protein kinase exaggerates high fat diet-induced cardiac hypertrophy and contractile dysfunction. *J Mol Cell Cardiol* **50**, 712–722.
 - 17 Ren J (2004) Leptin and hyperleptinemia – from friend to foe for cardiovascular function. *J Endocrinol* **181**, 1–10.
 - 18 Bagchi DP and MacDougald OA (2019) Identification and dissection of diverse mouse adipose depots. *J Vis Exp*.
 - 19 Bargut TCL, Souza-Mello V, Aguila MB and Mandarim-de-Lacerda CA (2017) Browning of white adipose tissue: lessons from experimental models. *Horm Mol Biol. Clin Investig* **31**.
 - 20 Kleiner DE, Brunt EM, Van Natta M, Behling C, Contos MJ, Cummings OW, Ferrell LD, Liu Y-C, Torbenson MS, Unalp-Arida A *et al.* (2005) Design and validation of a histological scoring system for nonalcoholic fatty liver disease. *Hepatology* **41**, 1313–1321.
 - 21 Seidell JC and Halberstadt J (2015) The global burden of obesity and the challenges of prevention. *Ann Nutr Metab* **66**(Suppl 2), 7–12.
 - 22 Baskaran P, Markert L, Bennis J, Zimmerman L, Fox J and Thyagarajan B (2019) Assessment of pharmacology, safety, and metabolic activity of capsaicin feeding in mice. *Sci Rep* **9**, 8588.
 - 23 Garami A, Pakai E, Oliveira DL, Steiner AA, Wanner SP, Almeida MC, Lesnikov VA, Gavva NR and Romanovsky AA (2011) Thermoregulatory phenotype of the Trpv1 knockout mouse: thermoeffector dysbalance with hyperkinesia. *J Neurosci* **31**, 1721–1733.
 - 24 Wanner SP, Garami A and Romanovsky AA (2011) Hyperactive when young, hypoactive and overweight when aged: connecting the dots in the story about locomotor activity, body mass, and aging in Trpv1 knockout mice. *Aging (Albany NY)* **3**, 450–454.
 - 25 Hai J, Kawabata F, Uchida K, Nishimura S and Tabata S (2020) Intra-gastric administration of AMG517, a TRPV1 antagonist, enhanced activity-dependent energy metabolism via capsaicin-sensitive sensory nerves in mice. *Biosci Biotechnol Biochem* **84**, 2121–2127.
 - 26 Garami A, Shimansky YP, Pakai E, Oliveira DL, Gavva NR and Romanovsky AA (2010) Contributions of different modes of TRPV1 activation to TRPV1 antagonist-induced hyperthermia. *J Neurosci* **30**, 1435–1440.
 - 27 Garami A, Pakai E, McDonald HA, Reilly RM, Gomtsyan A, Corrigan JJ, Pinter E, Zhu DXD, Lehto SG, Gavva NR *et al.* (2018) TRPV1 antagonists that cause hypothermia, instead of hyperthermia, in rodents: compounds' pharmacological profiles, in vivo targets, thermoeffectors recruited, and implications for drug development. *Acta Physiol (Oxf)* **223**, e13038.
 - 28 Nash MS, McIntyre P, Groarke A, Lilley E, Culshaw A, Hallett A, Panesar M, Fox A and Bevan S (2012) 7-tert-Butyl-6-(4-chloro-phenyl)-2-thioxo-2,3-dihydro-1H-pyrido[2,3-d]pyrimidin-4-one, a classic polymodal inhibitor of transient receptor potential vanilloid type 1 with a reduced liability for hyperthermia, is analgesic and ameliorates visceral hypersensitivity. *J Pharmacol Exp Ther* **342**, 389–398.
 - 29 Brown W, Leff RL, Griffin A, Hossack S, Aubray R, Walker P and Chiche DA (2017) Safety, pharmacokinetics, and pharmacodynamics study in healthy subjects of oral NEO6860, a modality selective transient receptor potential vanilloid subtype 1 antagonist. *J Pain* **18**, 726–738.
 - 30 Damann N, Bahrenberg G, Stockhausen H, Habermann CJ, Lesch B, Frank-Foltyn R, Lee J, Ann J and Christoph T (2020) In vitro characterization of the thermoneutral

- transient receptor potential vanilloid-1 (TRPV1) inhibitor GRTE16523. *Eur J Pharmacol* **871**, 172934.
- 31 Yoshida A, Furube E, Mannari T, Takayama Y, Kittaka H, Tominaga M and Miyata S (2016) TRPV1 is crucial for proinflammatory STAT3 signaling and thermoregulation-associated pathways in the brain during inflammation. *Sci Rep* **6**, 26088.
- 32 Obi S, Nakajima T, Hasegawa T, Kikuchi H, Oguri G, Takahashi M, Nakamura F, Yamasoba T, Sakuma M, Toyoda S *et al.* (2016). Heat induces interleukin-6 in skeletal muscle cells via TRPV1/PKC/CREB pathways. *J Appl Physiol (1985)* **122**, 683–694.
- 33 Farmer SR (2005) Regulation of PPAR[[gamma]] activity during adipogenesis. *Int J Obesity* **29**, S13–S16.
- 34 Contreras AV, Torres N and Tovar AR (2013) PPAR- α as a key nutritional and environmental sensor for metabolic adaptation. *Adv Nutrition* **4**, 439–452.
- 35 Smith SA (2002) Peroxisome proliferator-activated receptors and the regulation of mammalian lipid metabolism. *Biochem Soc Trans* **30**, 1086–1090.
- 36 Rachid TL, Penna-de-Carvalho A, Bringhenti I, Aguila MB, Mandarim-de-Lacerda CA and Souza-Mello V (2015) PPAR-alpha agonist elicits metabolically active brown adipocytes and weight loss in diet-induced obese mice. *Cell Biochem Funct* **33**, 249–256.
- 37 Brenner R, Baskaran P and Thyagarajan B (2018) Regulation of TRPV1 expression in non-neuronal tissues by BDNF, Sp1, and Sp4. *Biophys J* **114**, 17–21.
- 38 Ornellas F, Souza-Mello V, Mandarim-de-Lacerda CA and Aguila MB (2015) Programming of obesity and comorbidities in the progeny: lessons from a model of diet-induced obese parents. *PLoS One* **10**, e0124737.
- 39 Guijarro de Armas MG, Monereo Megias S, Navea Aguilera C, Merino Viveros M and Vega Pinero MB (2015) Non-alcoholic fatty liver in children and adolescents with excess weight and obesity. *Med Clin (Barc)* **144**, 55–58.
- 40 Kim D and Kim WR (2017) Nonobese fatty liver disease. *Clin Gastroenterol Hepatol* **15**, 474–485.

Supporting information

Additional supporting information may be found online in the Supporting Information section at the end of the article.

Fig. S1. Organ/tissue weights of NCD or HFD-fed WT and TRPV1^{-/-} mice.

Fig. S2. Agarose gel picture for genotyping TRPV1^{-/-} mice. Representative image of 1% agarose gel.